INTERNATIONAL JOURNAL FOR NUMERICAL METHODS IN FLUIDS
Int. J. Numer. Meth. Fluids 2002; **40**:1381–1400 (DOI: 10.1002/fld.414)

Energy dynamics in a turbulent channel flow using the Karhunen-Loéve approach

G. A. Webber[1,*,†], R. A. Handler[2] and L. Sirovich[3]

[1]*Center for Fluid Mechanics, Brown University, Providence, RI 02912*
[2]*Naval Research Laboratory, Washington, DC 20375, U.S.A.*
[3]*Laboratory of Applied Mathematics, Mount Sinai School of Medicine, New York, NY 10029, U.S.A.*

SUMMARY

The dynamical equations for the energy in a turbulent channel flow have been developed by using the Karhunen-Loéve modes to represent the velocity field. The energy balance equations show that all the energy in the flow originates from the applied pressure gradient acting on the mean flow. Energy redistribution occurs through triad interactions, which is basic to understanding the dynamics. Each triad interaction determines the rate of energy transport between source and sink modes via a catalyst mode. The importance of the proposed method stems from the fact that it can be used to determine both the rate of energy transport between modes as well as the direction of energy flow. The effectiveness of the method in determining the mechanisms by which the turbulence sustains itself is demonstrated by performing a detailed analysis of triad interactions occurring during a turbulent burst in a minimal channel flow. The impact on flow modification is discussed. Copyright © 2002 John Wiley & Sons, Ltd.

KEY WORDS: Karhunen-Loéve; wall-bounded turbulent flow; energy balance analysis

1. INTRODUCTION

Wall-bounded turbulent flows are of obvious technological significance and include very basic ones such as turbulent boundary layer flows over plane surfaces, flows in conduits (pipes, channels), as well as flows over surfaces possessing complex geometries. A large body of experimental work has revealed that although these flows vary randomly in time and space, they appear to possess quasi-deterministic coherent structures [1, 2]. Recently, direct simulations of these flows at low Reynolds numbers have been used to more rigorously define and understand the nature of these coherent structures [3–5]. Other related work has

* Correspondence to: G. A. Webber, SKY Computers, Chelmsford, MA 01821, U.S.A.
† E-mail: awebber@netway.com

Contract/grant sponsor: Office of Naval Research

Received 1 November 2000
Revised 2 May 2002

been motivated by the goal of generating a low-order dynamical system for wall bounded turbulence [6–8].

Previously Webber *et al.* [9], hereafter referred to as WHS, investigated a fully developed turbulent channel flow using the Karhunen-Loéve (KL) methodology to explore its dynamics. In that work the KL method, which will be described briefly below, was applied to the so-called *minimal channel* flow [10] whose dynamics are known to be somewhat simpler, but quite representative of wall bounded turbulence obtained in larger domains. In the previous work (WHS) it was shown that it was useful to interpret each KL mode as having physical significance. In particular, it was found useful to divide the modes into those which represent the mean flow (net flux modes) and those which can be associated with dynamical structures which exchange energy with the mean, referred to as roll modes and propagating modes. During a turbulent burst, it was found that the roll and propagating modes gained energy in a particular temporal order. However, it was evident that the KL analysis alone could not determine the *direction* of energy flow between modes through non-linear interactions. However, since drag increases during a turbulent burst, knowledge of which modes give up energy to other modes may be of importance in devising strategies to inhibit such interactions and thereby reduce drag. In addition, since the KL modes themselves satisfy incompressibility and the boundary conditions, the equations describing energy transport between modes can be considerably simplified. This leads to a streamlining of the numerical procedures and may also lead to greater insight into the flow dynamics. Our principal aim in this work is to describe the formulation of the energy transport problem using KL modes and to illustrate its utility by applying it to turbulent channel flow.

The phenomenology associated with wall bounded turbulence, such as the ejection-burst-sweep cycle, is described in WHS and will not be described further here. On the other hand, it is useful in the context of this work, to think of the problem in global terms as an input–output problem. In particular, for a given driving pressure gradient there will be a resultant steady-state mass flux. In turbulent channel flow driven by a predetermined constant pressure gradient, the mass flux is much reduced compared to that of a laminar flow for the same pressure gradient. Thus, the turbulence is effectively extracting energy from the mean flow in order to maintain itself. It will be shown below that formulating the energy transport problem in terms of the KL modes can shed some light on the non-linear energy transport process which maintains the turbulence and ultimately results in drag.

2. TURBULENCE SIMULATION AND KL PROCEDURE

2.1. Turbulence simulation

We simulate the flow in a channel driven by a uniform pressure gradient by solving the incompressible Navier–Stokes equations which in normalized form are given by

$$\frac{\partial \mathbf{U}}{\partial t} = -\mathbf{U} \cdot \boldsymbol{\nabla}\mathbf{U} - \boldsymbol{\nabla} p + \frac{1}{R_\tau}\nabla^2 \mathbf{U} + 1\mathbf{e}_1 \tag{1}$$

$$\boldsymbol{\nabla} \cdot \mathbf{U} = 0 \tag{2}$$

together with the no slip boundary conditions given by

$$\mathbf{U} = 0, \quad x_2 = \pm 1 \tag{3}$$

where $\mathbf{U}(\mathbf{x},t)$ is the velocity, and p is the pressure. The Reynolds number is given by $R_\tau = u_\tau h/\nu$, where ν is the kinematic viscosity, h is the channel half-width, and the friction velocity $u_\tau = \sqrt{\tau_w/\rho} = \sqrt{kh/\rho}$, where τ_w is the viscous shear stress at one wall, k is the constant driving pressure gradient, and ρ is the density. In the equations above, velocity, pressure, length, and time are made non-dimensional by u_τ, ρu_τ^2, h, and h/u_τ, respectively. The applied pressure gradient is constant and in this normalization is given by $1\mathbf{e}_1$ where $\mathbf{e}_1$ is the unit vector in the streamwise direction.

We use the notation (x_1, x_2, x_3) to denote the streamwise, wall normal, and spanwise coordinates, respectively. The superscript $(+)$ is taken to imply a velocity, length, or time normalized by u_τ, ν/u_τ, and ν/u_τ^2 respectively. The flow is assumed to be periodic in the x_1 and x_3 directions with corresponding domain lengths of $L_1 = \pi h$ and $L_3 = 0.3 \times \pi h$. The resolution was $129 \times 48 \times 24$ in the wall normal, streamwise and spanwise directions, respectively. The friction Reynolds number R_τ was set to 135.5 which was so chosen as to maintain a bulk Reynolds number, $Re_b = \frac{3}{2}\langle U_b \rangle h/\nu = 3000$, as determined from the results of Dean [11] where the bulk velocity U_b is given by

$$U_b(t) = \frac{1}{A}\int_A \mathbf{U}(\mathbf{x},t)\,\mathrm{d}A \tag{4}$$

where $A = 2L_3 h$ is the cross-sectional area and $\langle\,\rangle$ represents time averaging. Further details about the numerical simulation can be found elsewhere [12, 13].

The kinetic energy of the flow is defined by

$$E(t) = \frac{1}{2V}\int_V \mathbf{U}(\mathbf{x},t)\cdot\mathbf{U}(\mathbf{x},t)\,\mathrm{d}\mathbf{x} \tag{5}$$

so that the rate of change of the energy in the system is given by

$$\frac{\mathrm{d}}{\mathrm{d}t}E(t) = \frac{1}{V}\int_V \mathbf{U}(\mathbf{x},t)\cdot\frac{\partial}{\partial t}\mathbf{U}(\mathbf{x},t)\,\mathrm{d}\mathbf{x} \tag{6}$$

Substitution of the equations of motion into (6) gives (see Appendix A.1)

$$\frac{\mathrm{d}}{\mathrm{d}t}E(t) = \frac{-1}{V\,Re_\tau}\int_V (\nabla\mathbf{U}_i)^2\,\mathrm{d}\mathbf{x} + \frac{1}{V}\int_V \mathbf{U}\cdot\mathbf{e}_1\,\mathrm{d}\mathbf{x} \tag{7}$$

The viscous term is always negative so that viscosity acts as an energy sink. The term involving the applied pressure gradient must be positive (unless the bulk velocity suddenly becomes negative) and acts as the sole energy source for the system. Non-linear convective terms and pressure–velocity interactions which act only to redistribute the kinetic energy (see Appendix A.1), vanish in the net energy balance given by (7).

2.2. *Karhunen-Loéve decomposition*

In this paper the Karhunen-Loéve or proper orthogonal decomposition (POD) procedure is applied to the turbulent channel flow described above. Only the rudiments of the method are

included here and descriptions of greater detail can be found elsewhere [14–16]. Since the velocity field is periodic in the x_1 and x_3 directions, a K-L analysis can be performed on $\mathbf{u}(x_2, m, n)$ which is the Fourier transform of $\mathbf{U}$ in the horizontal (x_1 and x_3) plane, where m and n correspond to the streamwise and spanwise wavenumber indices, respectively. The analysis reported in this paper was performed *without* removing the mean velocity field. The empirical eigenfunctions, $\boldsymbol{\psi}$, and eigenvalues, λ, are determined from the equation:

$$\int_{-1}^{1} \kappa_{ij}(x_2, x_2', m, n)\psi_j(x_2', m, n)\,\mathrm{d}x_2' = \lambda(m, n)\psi_i(x_2), \quad i, j = 1, 2, 3 \tag{8}$$

where $\kappa_{ij}(x_2, x_2', m, n)$ is the two-point spatial correlation tensor or covariance matrix formed from

$$\kappa_{ij}(x_2, x_2', m, n) = \langle u_i(x_2, m, n)\bar{u}_j(x_2', m, n)\rangle \tag{9}$$

where the overbar denotes complex conjugation, and expectation is taken over all realizations and flow symmetries [16]. The three-dimensional eigenfunction is a complex valued vector field which can be written as

$$\boldsymbol{\phi}^{\mathbf{k}}(x_1, x_2, x_3) = \boldsymbol{\phi}^{(m,n,q)}(x_1, x_2, x_3) = \boldsymbol{\psi}^{q}(x_2, m, n)\mathrm{e}^{2\pi \mathrm{i} m x_1/L_1}\mathrm{e}^{2\pi \mathrm{i} n x_3/L_3} \tag{10}$$

We use the triplet $\mathbf{k} = (m, n, q)$ to completely specify the eigenfunction $\boldsymbol{\phi}^{\mathbf{k}}$.

It is important to note several important features of the eigenmodes which are useful for the analysis undertaken here. First, since the eigenfunctions are derived from physical flow fields, they are themselves flow fields and retain the incompressibility property, $\boldsymbol{\nabla} \cdot \boldsymbol{\phi}^{\mathbf{k}} = 0$. In addition, they satisfy the no slip boundary condition, $\boldsymbol{\phi}^{\mathbf{k}} = 0$ at $x_2 = \pm 1$. Secondly, it follows from the Hermitian property of $\kappa_{ij}(x_2, x_2', m, n)$ that the eigenfunctions can be made orthonormal:

$$\frac{1}{V}\int_V \boldsymbol{\phi}^{\mathbf{k}} \cdot \bar{\boldsymbol{\phi}}^{\mathbf{l}}\,\mathrm{d}\mathbf{x} = \delta_{\mathbf{kl}} \tag{11}$$

and it can be further shown that the eigenvalues are real and non-negative. Once obtained, the velocity field can be represented as a sum of the eigenfunctions as follows:

$$\mathbf{U}(\mathbf{x}, t) = \sum_{\mathbf{k}} a^{\mathbf{k}}(t)\boldsymbol{\phi}^{\mathbf{k}}(\mathbf{x}) \tag{12}$$

where the K-L coefficients are obtained from

$$a^{\mathbf{k}}(t) = \frac{1}{V}\int_V \mathbf{U}(\mathbf{x}, t) \cdot \bar{\boldsymbol{\phi}}(\mathbf{x})^{\mathbf{k}}\,\mathrm{d}\mathbf{x} \tag{13}$$

The eigenmodes chosen in this way converge optimally in the mean square sense to the original data [14, 16].

In previous work [4, 5, 9] it was found useful to separate the KL modes into groups for which some physical significance could be attached. The so-called *net flux* modes are those with zero streamwise and spanwise wavenumbers. As such, they represent the modes which

correspond to the instantaneous horizontally averaged velocity profile and are the only modes which can represent the mass flux through the channel. The most energetic mode in this group which very closely approximates the average flow field and composes the bulk of the energy in the flow is referred to as the *mother* mode. Modes with spanwise dependence but no streamwise dependence are referred to as *roll* modes. The most energetic modes in this group (see WHS) have a spanwise spacing of about $100v/u_\tau$, the length scale associated with the so-called boundary layer streaky structures [1, 17]. Modes with streamwise dependence are referred to as *propagating* modes since members of the group appear to have wave-like character [4, 5]. The more energetic propagating modes appear similar in form to inclined streamwise vortices which are often found in the turbulent boundary layer [18, 19]. Visualizations of these modes and their relationship to experimental observations are found in WHS.

3. THE ENERGY TRANSPORT EQUATIONS FOR A TURBULENT FLOW USING KL MODES AS A BASIS

The principal goal of this work is to develop a method of tracking the flow of energy between modes of a turbulent system by taking advantage of the properties of the KL modes discussed above. To proceed, an expression for the time rate of change of the energy for each individual KL mode is required. Using the orthogonality properties of the eigenmodes, it can be shown (see Appendix A.2) that the energy of the system can be expressed in terms of the time dependent coefficients $a^{\mathbf{k}}(t)$ as follows:

$$E(t) = \frac{1}{2V}\int_V \mathbf{U}\cdot\mathbf{U}\,\mathrm{d}\mathbf{x} = \sum_{\mathbf{k}} \frac{1}{2}\, a^{\mathbf{k}}(t)\vec{a}^{\mathbf{k}}(t) = \sum_{\mathbf{k}} E^{\mathbf{k}}(t) \tag{14}$$

Here the energy in any *individual* KL mode is defined as

$$E^{\mathbf{k}}(t) = \frac{1}{2} a^{\mathbf{k}}(t)\vec{a}^{\mathbf{k}}(t) \tag{15}$$

and its time rate of change can be written:

$$\frac{\mathrm{d}}{\mathrm{d}t} E^{\mathbf{k}} = \frac{1}{2}\left(\vec{a}^{\mathbf{k}}(t)\frac{\mathrm{d}}{\mathrm{d}t} a^{\mathbf{k}}(t)\right) \tag{16}$$

where it is understood that since the energy is real, the complex conjugate must be added to the above expression. The operation of adding the complex conjugate to insure positivity will be implicit in the derivations to follow.

In addition to quantity of energy, the distribution of energy is also important. The portion of energy in each mode can be calculated by the equation $p^{\mathbf{k}}(t) = E^{\mathbf{k}}(t)/\sum_{\mathbf{k}'} E^{\mathbf{k}'}(t)$, so that $p^{\mathbf{k}}(t)$ is a probability. Finally a representational entropy, $S(t)$, is calculated which measures the degree to which the energy is distributed over the modes:

$$S(t) = -\sum p^{\mathbf{k}}(t)\ln(p^{\mathbf{k}}(t)) \tag{17}$$

A small value of S indicates that few modes contain the bulk of the energy while a large value of S indicates that the energy is distributed over many modes. While the flow can

be represented by any orthonormal basis set, it has been shown by Sirovich [16] that the empirical eigenfunctions are the basis which minimizes the representational entropy for the time averaged probabilities.

The expression for time rate of change of the coefficients, which is determined by introducing expansion (12) into the equations of motion (1), multiplying by $\bar{\boldsymbol{\phi}}^{\mathbf{k}}$, and integrating over the volume, is given by

$$\frac{\mathrm{d}}{\mathrm{d}t}a^{\mathbf{k}}(t) = -\sum_{\mathbf{k}'}\sum_{\mathbf{k}''}a^{\mathbf{k}'}a^{\mathbf{k}''}\beta^{\mathbf{k}\mathbf{k}'\mathbf{k}''} + \frac{1}{R_\tau}\sum_{\mathbf{k}'}a^{\mathbf{k}'}\varepsilon^{\mathbf{k}\mathbf{k}'} + \eta^{\mathbf{k}} \tag{18}$$

where

$$\beta^{\mathbf{k}\mathbf{k}'\mathbf{k}''} = \frac{1}{V}\int_V \bar{\boldsymbol{\phi}}^{\mathbf{k}} \cdot (\boldsymbol{\phi}^{\mathbf{k}'} \cdot \boldsymbol{\nabla}\boldsymbol{\phi}^{\mathbf{k}''})\,\mathrm{d}\mathbf{x} \tag{19}$$

$$\varepsilon^{\mathbf{k}\mathbf{k}'} = \frac{1}{V}\int_V \bar{\boldsymbol{\phi}}^{\mathbf{k}} \cdot \boldsymbol{\nabla}^2\boldsymbol{\phi}^{\mathbf{k}'}\,\mathrm{d}\mathbf{x} \tag{20}$$

$$\eta^{\mathbf{k}} = \frac{1}{V}\int_V \bar{\boldsymbol{\phi}}^{\mathbf{k}} \cdot \mathbf{e}_1\,\mathrm{d}\mathbf{x} \tag{21}$$

Introducing (18) into (16) yields an expression for the time rate of change of the energy as follows:

$$\frac{\mathrm{d}}{\mathrm{d}t}E^{\mathbf{k}}(t) = \frac{1}{2}\left(-\bar{a}^{\mathbf{k}}\sum_{\mathbf{k}'}\sum_{\mathbf{k}''}a^{\mathbf{k}'}a^{\mathbf{k}''}\beta^{\mathbf{k}\mathbf{k}'\mathbf{k}''} + \bar{a}^{\mathbf{k}}\frac{1}{R_\tau}\sum_{\mathbf{k}'}a^{\mathbf{k}'}\varepsilon^{\mathbf{k}\mathbf{k}'} + \bar{a}^{\mathbf{k}}\eta^{\mathbf{k}}\right) \tag{22}$$

The coefficients $\beta^{\mathbf{k}\mathbf{k}'\mathbf{k}''}$, $\varepsilon^{\mathbf{k}\mathbf{k}'}$, and $\eta^{\mathbf{k}}$ are time independent and can be computed, once and for all, using the known KL eigenfunctions. As noted earlier, since the KL eigenfunctions satisfy continuity and the boundary conditions, the expression for the evolution of the energy derived from them does not involve pressure terms.

We now consider the significance of the individual terms in the energy balance. The energy input to any KL mode from the applied pressure gradient is given by the term involving $\eta^{\mathbf{k}}$. Since each eigenfunction is a product of complex exponentials in the streamwise and spanwise directions it follows that $\eta^{\mathbf{k}}$ will be zero for all modes other than the net flux modes for which $m = n = 0$. The energy input to the system can then be calculated as follows:

$$\frac{\mathrm{d}}{\mathrm{d}t}E(t)_{\text{input}} = \frac{1}{V}\int_V \mathbf{U} \cdot \mathbf{e}_1\,\mathrm{d}\mathbf{x} = \sum_{\mathbf{k}}\left(\frac{\mathrm{d}}{\mathrm{d}t}E^{\mathbf{k}}(t)\right)_{\eta^{\mathbf{k}}} = \frac{1}{2}\sum_q \bar{a}^{(0,0,q)}\eta^{(0,0,q)} \tag{23}$$

where the term $((\mathrm{d}/\mathrm{d}t)E^{\mathbf{k}}(t))_{\eta^{\mathbf{k}}}$ represents the change in the term $E^{\mathbf{k}}(t)$ due to the term $\eta^{\mathbf{k}}$. The system can therefore receive energy only through the pressure gradient acting on the net flux modes. The average time rate of change of energy $C^{\mathbf{k}}$ due to this term is defined as follows:

$$C^{\mathbf{k}} = \frac{1}{T}\int_0^T \bar{a}^{\mathbf{k}}(t)\eta^{\mathbf{k}}\,\mathrm{d}t = \langle \bar{a}^{\mathbf{k}} \rangle \eta^{\mathbf{k}} \tag{24}$$

Each KL mode loses energy to viscosity as embodied in the term involving $\varepsilon^{\mathbf{k}\mathbf{k}'}$. The energy loss of the system can therefore be expressed by

$$\frac{\mathrm{d}}{\mathrm{d}t}E(t)_{\text{output}} = \frac{1}{V\,Re_\tau}\int_V \mathbf{U}\cdot\nabla^2\mathbf{U}\,\mathrm{d}\mathbf{x}$$
$$= \frac{1}{Re_\tau}\sum_{\mathbf{k}}\sum_{\mathbf{k}'}\left(\frac{\mathrm{d}}{\mathrm{d}t}E^{\mathbf{k}}(t)\right)_{\varepsilon^{\mathbf{k}\mathbf{k}'}} = \frac{1}{2R_\tau}\left(\sum_{\mathbf{k}}\sum_{\mathbf{k}'}\bar{a}^{\mathbf{k}}(t)a^{\mathbf{k}'}(t)\varepsilon^{\mathbf{k}\mathbf{k}'}\right) \tag{25}$$

where $((\mathrm{d}/\mathrm{d}t)E^{\mathbf{k}}(t))_{\varepsilon^{\mathbf{k}\mathbf{k}'}}$ represents the change in $E^{\mathbf{k}}$ due to the $\varepsilon^{\mathbf{k}\mathbf{k}'}$ term. The mean rate at which each mode loses energy to viscosity is given by

$$L^{\mathbf{k}} = \left\langle\left(\frac{\mathrm{d}}{\mathrm{d}t}E^{\mathbf{k}}(t)\right)_{\varepsilon}\right\rangle = \frac{1}{2\,Re_\tau}\left(\sum_{\mathbf{k}'}\langle\bar{a}^{\mathbf{k}}a^{\mathbf{k}'}\rangle\varepsilon^{\mathbf{k}\mathbf{k}'}\right) \tag{26}$$

Since the KL coefficients are uncorrelated [16], that is $\langle\bar{a}^{\mathbf{k}}a^{\mathbf{k}'}\rangle = \lambda^{\mathbf{k}}\delta^{\mathbf{k}\mathbf{k}'}$, it follows that

$$L^{\mathbf{k}} = \frac{1}{2\,Re_\tau}\lambda^{\mathbf{k}}\varepsilon^{\mathbf{k}\mathbf{k}} \tag{27}$$

Since it can be shown that $\varepsilon^{\mathbf{k}\mathbf{k}}$ is real and *negative* (see Appendix A.2) and that the eigenvalues must always be positive, the expected result that viscosity can only drain energy from each mode is derived.

The term involving $\beta^{\mathbf{k}\mathbf{k}'\mathbf{k}''}$, which originates from the non-linear convective term in the original equations of motion, represents the transport of energy between modes due to the so-called *triad* interactions. It is important to note that these terms will contribute no *net* energy to the system. The nature of these terms arises from the fact that $\beta^{\mathbf{k}\mathbf{k}'\mathbf{k}''}$ will be zero unless $m' + m'' - m = 0$ and $n' + n'' - n = 0$ (see Appendix A.2). When these conditions are met, the modes are said to form a triad. The rate of energy increase to mode $\mathbf{k}$ by the triad $(\mathbf{k}, \mathbf{k}', \mathbf{k}'')$ can be written as

$$\left(\frac{\mathrm{d}}{\mathrm{d}t}E^{\mathbf{k}}(t)\right)_{\beta^{\mathbf{k}\mathbf{k}'\mathbf{k}''}} = \frac{1}{2}(-\bar{a}^{\mathbf{k}}a^{\mathbf{k}'}a^{\mathbf{k}''}\beta^{\mathbf{k}\mathbf{k}'\mathbf{k}''}) \tag{28}$$

Important symmetry properties associated with the triad terms can be derived by first noting that if $\mathbf{k}\mathbf{k}'\mathbf{k}''$ forms a triad, then $\mathbf{k}''\bar{\mathbf{k}}'\mathbf{k}$ also forms a triad, where $\bar{\mathbf{k}}'$ refers to the triplet $(-m', -n', q')$. It follows (see Appendix A.2) that

$$\left(\frac{\mathrm{d}}{\mathrm{d}t}E^{\mathbf{k}}(t)\right)_{\beta^{\mathbf{k}\mathbf{k}'\mathbf{k}''}} = -\left(\frac{\mathrm{d}}{\mathrm{d}t}E^{\mathbf{k}''}(t)\right)_{\beta^{\mathbf{k}''\bar{\mathbf{k}}'\mathbf{k}}} \tag{29}$$

This relation implies that, if the energy in mode $\mathbf{k}$ is *increasing* due to a given triad, the mode $\mathbf{k}''$ *loses* energy at the same rate. Thus, for any given triad, $\mathbf{k}$ and $\mathbf{k}''$ can always be identified as either sources or sinks, and the given intermediate mode $\mathbf{k}'$ which gains no *net* energy from this triad during the interaction, is referred to as a *catalyst*. The average rate at

which energy is transported to or from mode $\mathbf{k}$ by a given triad is defined by

$$T^{\mathbf{k}\mathbf{k}'\mathbf{k}''} = \frac{1}{2}(\langle -\bar{a}^{\mathbf{k}} a^{\mathbf{k}'} a^{\mathbf{k}''} \rangle \beta^{\mathbf{k}\mathbf{k}'\mathbf{k}''}) \tag{30}$$

If $T^{\mathbf{k}\mathbf{k}'\mathbf{k}''}$ is positive, then this triad represents energy flowing from mode $\mathbf{k}''$ to mode $\mathbf{k}$.

It is convenient in what follows to define *primary* triads as those in which the mother mode ($\mathbf{k} = (0, 0, 1)$) is involved. This is because the mother mode, which contains approximately 90% of the flow energy, receives the bulk of its energy from the mean pressure gradient and in turn acts as the source for the most energetic triads. Triads not involving the mother mode will be referred to as *secondary* triads.

We can simplify the analysis of the flow energetics by defining energy transport among groups of modes. As an example, the rate of energy flow from the net flux (NF) modes to the roll (R) modes due to triad interactions is calculated by adding the energy flow among all triads where the net flux modes are the $\mathbf{k}''$ modes and the roll modes are the $\mathbf{k}$ modes as follows:

$$\left(\frac{\mathrm{d}}{\mathrm{d}t}E(t)\right)_{NF\to R} = \frac{-1}{2} \sum_{\substack{\mathbf{k} \\ m=0 n\neq 0}} \sum_{\mathbf{k}'} \sum_{\substack{\mathbf{k}'' \\ m''=0 n''=0}} \bar{a}^{\mathbf{k}}(t) a^{\mathbf{k}'}(t) a^{\mathbf{k}''}(t) \beta^{\mathbf{k}\mathbf{k}'\mathbf{k}''} \tag{31}$$

In a similar manner the triad interactions between net flux and propagating modes and between roll and propagating modes are also computed as follows:

$$\left(\frac{\mathrm{d}}{\mathrm{d}t}E(t)\right)_{NF\to P} = \frac{-1}{2} \sum_{\substack{\mathbf{k} \\ m\neq 0}} \sum_{\mathbf{k}'} \sum_{\substack{\mathbf{k}'' \\ m''=0 n''=0}} \bar{a}^{\mathbf{k}}(t) a^{\mathbf{k}'}(t) a^{\mathbf{k}''}(t) \beta^{\mathbf{k}\mathbf{k}'\mathbf{k}''} \tag{32}$$

$$\left(\frac{\mathrm{d}}{\mathrm{d}t}E(t)\right)_{R\to P} = \frac{-1}{2} \sum_{\substack{\mathbf{k} \\ m\neq 0}} \sum_{\mathbf{k}'} \sum_{\substack{\mathbf{k}'' \\ m''=0 n''\neq 0}} \bar{a}^{\mathbf{k}}(t) a^{\mathbf{k}'}(t) a^{\mathbf{k}''}(t) \beta^{\mathbf{k}\mathbf{k}'\mathbf{k}''} \tag{33}$$

4. RESULTS FOR THE TRANSPORT TERMS IN THE ENERGY EQUATION

Turbulence in a minimal channel, as defined in Section 2, was simulated over a time period $t^+ = 4000$. The turbulence statistics, described in detail in WHS, are found to be in good agreement with the earlier results of Jimenez and Moin [10]. Realizations of the flow are then used to compute the KL modes as described earlier. The most energetic KL mode is found to be the mother mode which approximates the time averaged mean velocity profile. The next two most energetic modes are roll modes which account for 23.8% of the remaining turbulent energy, that is 23.8% of the energy not accounted for by the mother mode.

The time-dependent coefficients $a^{\mathbf{k}}(t)$ are computed by projecting the *known* KL eigenfunctions onto a second channel flow simulation. These coefficients are computed *on the fly*—simultaneously with the simulation—so as to avoid having to store further three-dimensional flow field realizations which were needed originally to compute the KL eigenfunctions. Time-dependent coefficients are computed and stored for 3025 modes which represent about 96.4% of the flow energy outside the mother mode or 99.64% of the total energy.

Table I. Energy transfer rate of the 10 most energetic triads in the minimal channel flow involving energy exchange with the mother mode.

Index	Sink mode (m,n,q)	Catalyst mode (m',n',q')	Source mode (m'',n'',q'')	$T^{\mathbf{k}\mathbf{k}'\mathbf{k}''}$
1	(0, 1, 2)	(0, 1, 2)	(0, 0, 1)	3.12809
2	(0, 1, 1)	(0, 1, 1)	(0, 0, 1)	2.88146
3	(0, 2, 2)	(0, 2, 2)	(0, 0, 1)	0.37905
4	(0, 2, 1)	(0, 2, 1)	(0, 0, 1)	0.36726
5	(1, 1, 1)	(1, 1, 1)	(0, 0, 1)	0.35512
6	(1, 1, 2)	(1, 1, 2)	(0, 0, 1)	0.34488
7	(0, 1, 3)	(0, 1, 3)	(0, 0, 1)	0.31349
8	(0, 1, 4)	(0, 1, 4)	(0, 0, 1)	0.27835
9	(1, 2, 2)	(1, 2, 2)	(0, 0, 1)	0.21905
10	(1, 2, 1)	(1, 2, 1)	(0, 0, 1)	0.18489

The KL coefficients computed as described above are the *exact* coefficients. Once they have been obtained, their time rate of change can be computed using a centre differencing scheme. On the other hand, the time rate of change of the coefficients can also be computed using (18)—that is, they are calculated *indirectly* from the Navier–Stokes equations. The indirectly computed time rate of change of the coefficients will differ from the exact rate of change since the source terms on the right-hand side of the governing equations are computed from the truncated set (3025 modes) of eigenmodes. We have compared the indirectly obtained time derivatives to the exact time derivatives for a representative set of coefficients and found that the rms difference between the two to be negligibly small. This gives us confidence that the set of coefficients and eigenfunctions used in this study are large enough to sufficiently represent the flow, and that the triad, viscous dissipation, and source terms are calculated correctly.

4.1. Computation of the dominant triads

Using the methods described above the energy transport due to selected triad interactions have been computed. $T^{\mathbf{k}\mathbf{k}'\mathbf{k}''}$ is used as a measure of the relative strength of each triad. The most energetic primary triads (triads involving the mother mode) have been ranked from largest to smallest in Table I. It is evident that the mother mode (the $(0,0,1)$ mode) acts as a source in the most energetic primary triads. In addition, the sink modes also act as their own catalysts. The two most energetic primary triads, whose energy transport rates are an order of magnitude larger than any other triads, involve energy transfer from the mother mode to the dominant roll modes. These two roll modes also rank as the most energetic KL modes (see WHS), other than the mother mode, in the sense that they have the largest mean square energy. The remaining sink modes listed in Table I also are among the most energetic KL modes. In examining the rate of transport ($T^{\mathbf{k}\mathbf{k}'\mathbf{k}''}$) for many triads, it appears that although many modes tend to receive the majority of their energy from modes other than the mother mode, the largest single source of energy for most modes is the mother mode with the sink acting as its own catalyst. The instantaneous rate of transport due to a triad as defined in (28) for the first triad listed in Table I is shown in Figure 1. We note that in this case, the energy flow is always positive, indicating that the energy always flows from the mother mode to

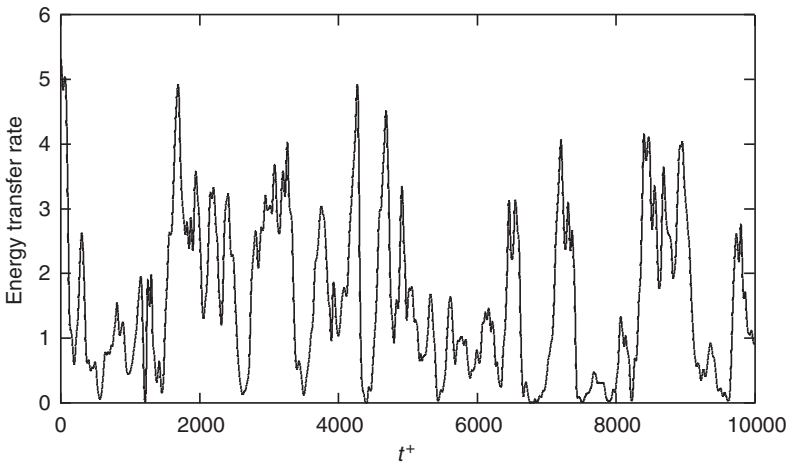

Figure 1. Energy transfer from the mother mode to the $(0,1,2)$ through the first triad.

Table II. Energy transfer rate of the 10 most energetic triads in the minimal channel flow not involving the mother mode.

Index	Sink mode (m,n,q)	Catalyst mode (m',n',q')	Source mode (m'',n'',q'')	$T^{\mathbf{k}\mathbf{k}'\mathbf{k}''}$
1	$(1,1,2)$	$(1,0,4)$	$(0,1,2)$	0.16340
2	$(0,2,2)$	$(0,1,2)$	$(0,1,2)$	0.15839
3	$(1,1,1)$	$(1,0,4)$	$(0,1,1)$	0.13536
4	$(0,0,3)$	$(0,1,1)$	$(0,1,1)$	0.12994
5	$(1,1,1)$	$(1,0,2)$	$(0,1,2)$	0.11070
6	$(0,2,1)$	$(0,1,1)$	$(0,1,2)$	0.10179
7	$(0,2,1)$	$(0,1,2)$	$(0,1,1)$	0.10004
8	$(0,2,2)$	$(0,1,1)$	$(0,1,1)$	0.09499
9	$(0,0,3)$	$(0,1,2)$	$(0,1,2)$	0.09081
10	$(1,1,2)$	$(1,0,2)$	$(0,1,1)$	0.08699

the $(0,1,2)$ mode. In general, however, it is always possible for the transport rates to change sign, indicating that a mode may switch chaotically from being a source to a sink.

A list of the most energetic secondary triads, which are those not involving the mother mode, are listed in Table II. Is is evident that roll modes are the sources for the most important secondary triads. Results from WHS show these roll modes to be significantly more energetic than any modes other the mother mode, and the fact that they are able to drive all of the dominant secondary triads is another confirmation of their importance in the dynamics. The most energetic secondary triad is associated with transport from the roll mode $(0,1,2)$ to the propagating mode $(1,1,2)$. In this case, while the average rate of transport associated with this triad is positive, Figure 2 shows that the transport actually goes the other way for brief time periods.

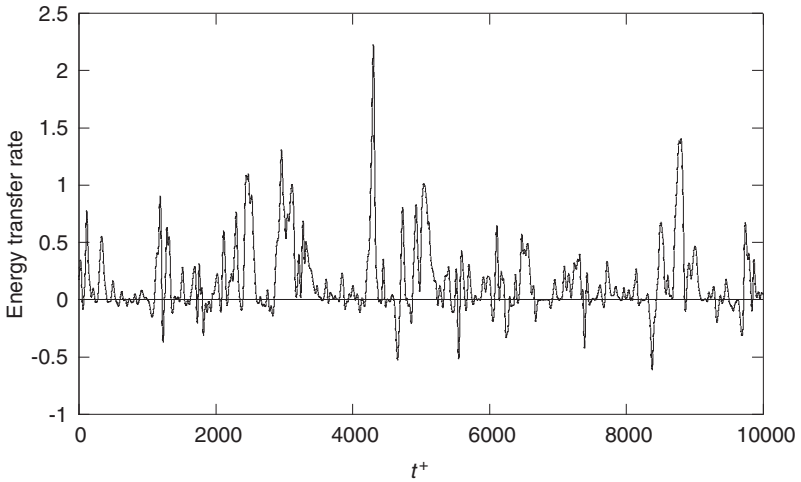

Figure 2. Energy transfer from $(0,1,2)$ mode to $(1,1,2)$ mode through most energetic secondary triad.

4.2. Group mode dynamics during a turbulent burst

An important observation, made in WHS, is that turbulent channel flow appears to undergo intermittent bursts of activity. Before such a burst, the mass flux and roll mode energy are seen to increase and the entropy reaches a minimum, indicating that relatively few modes carry most of the turbulent energy. One can view this part of the cycle as a tendency toward flow relaminarization. This is then followed abruptly by a rapid decrease in roll mode energy and mass flux, and an increase in propagating mode energy and entropy. We refer to these events as *entropy events*. In WHS the dynamical relationships between roll, propagating, and net flux modes could not be determined in detail since in that work triad transport rates were never computed. As is shown below, computation of the triad transport terms during these entropy events greatly clarifies our view of the dynamics.

The entropy events correspond to the local peaks in bulk velocity at times $t^+ \simeq 1000$ and $t^+ \simeq 4000$, which can be readily identified in Figure 3 along with the associated dips in entropy seen in Figure 4. We interpret these events as indicating that the flow is undergoing a weak relaminarization as the energy tends to be concentrated in fewer modes. A sharp rise in entropy is seen to follow a corresponding decrease in bulk velocity. One of the prime objectives of the present work is to describe the energy dynamics of such events, which is most easily done by considering the group dynamics.

To obtain an overall view of the dynamics during these entropy events, we sum the linear and non-linear interactions over the various mode groups—net flux modes, roll modes, and propagating modes defined in (31)–(33). The details of the triad interactions occurring among the various mode groups during a typical entropy event $(800 < t^+ < 1400)$ are given in Figures 5–8. It is useful in the following discussion to divide the event into three periods; $800 < t^+ < 1000$ (period one), $1000 < t^+ < 1150$ (period two), and $800 < t^+ < 1400$ (period three). During the first period, energy is transported almost exclusively *from* net flux modes to roll modes. For these interactions, the roll modes act as their own catalyst to draw energy from the mother mode through the primary triads. As a result, roll mode

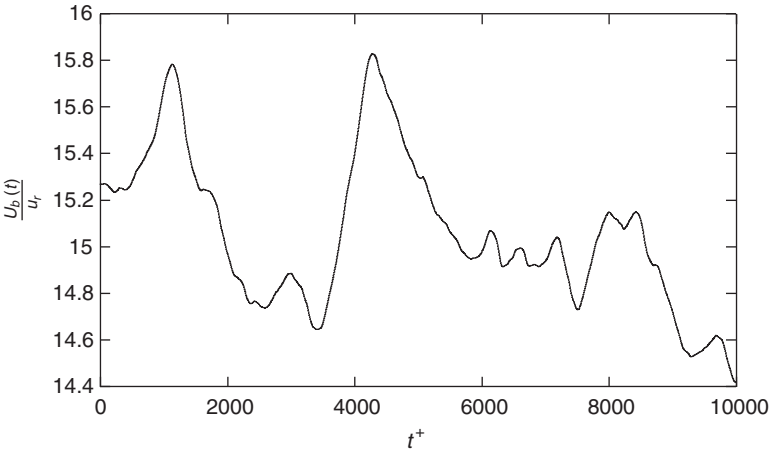

Figure 3. Bulk velocity of the minimal channel.

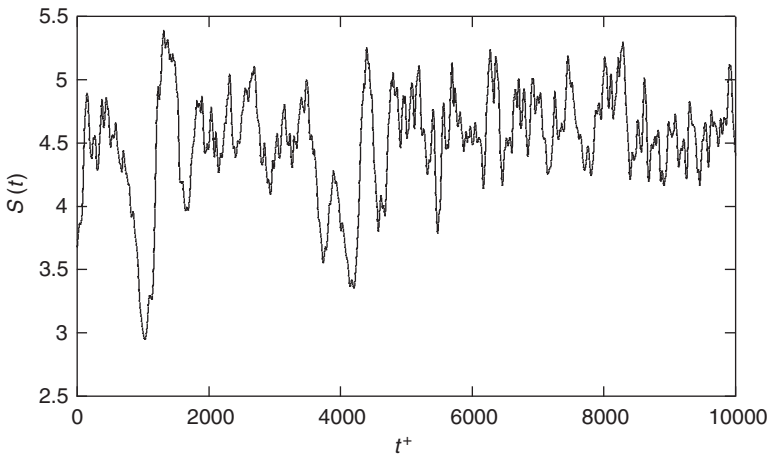

Figure 4. Representational entropy of minimal channel flow, $S(t)$.

energy increases rapidly while propagating mode energy remains stagnant as seen in Figures 5 and 6.

During the second period, the rate of energy transfer *from* the roll modes to the propagating modes shows a sharp increase. This transport results in a rapid rise in propagating mode energy as is evident in Figure 5. Towards the end of this period, the transport from net flux modes to roll modes decreases which results in a predictable decrease in roll mode energy. During the final period, energy is pumped into the propagating modes *directly* by the net flux modes as well as by the roll modes. This results in a rapid rise in propagating mode energy which corresponds to a dramatic increase in representational entropy seen in Figure 8. In summary, during the early stages of the event, the net flux modes drive the roll modes through primary

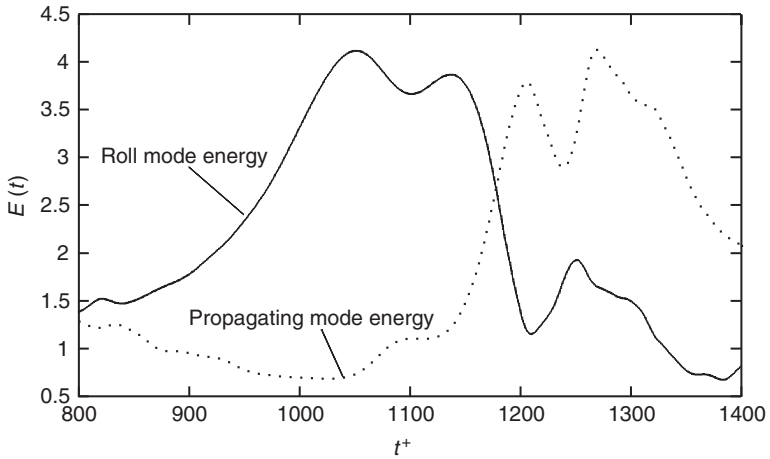

Figure 5. Energy in the mode groups. The solid line represents the energy in the roll modes and the dots represent the energy in the propagating modes.

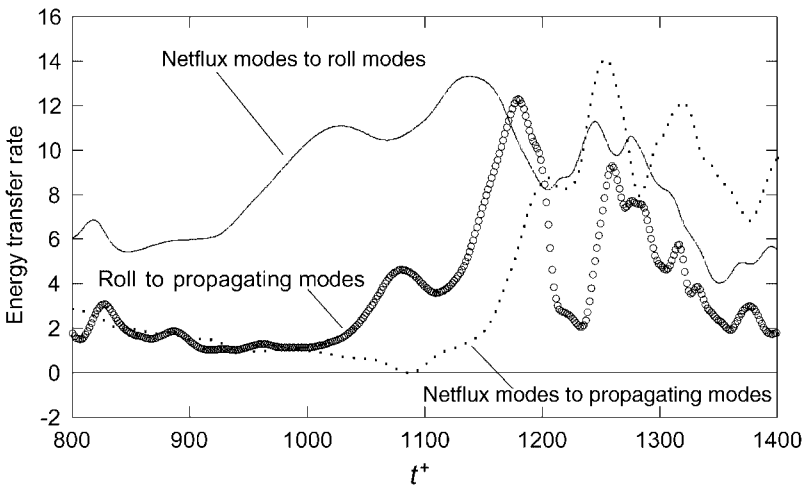

Figure 6. Energy transfer rate among mode groups. The solid line represents the transfer rate from the net flux modes to the roll modes as described in Equation (32). The dots represent net flux modes to propagating modes and the open circles represent roll modes to propagating modes.

triads—then secondary triads act to transfer energy from the roll modes to the propagating modes, and finally the net flux modes switch from driving roll modes to driving propagating modes.

It is important to note that in previous work it was not possible to determine with any certainty what processes were actually causing this bursting activity. The importance of the method described here is that we can not only determine which modes are interacting with each other, but also the *direction* of energy transport. As we describe below, this information

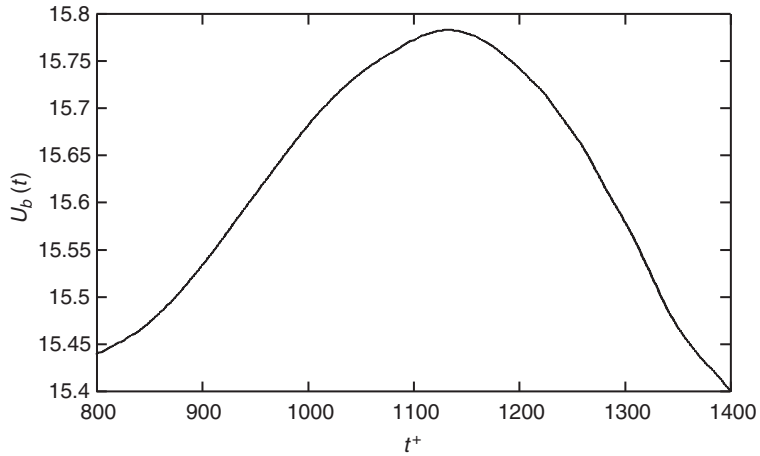

Figure 7. Bulk velocity during the entropy event.

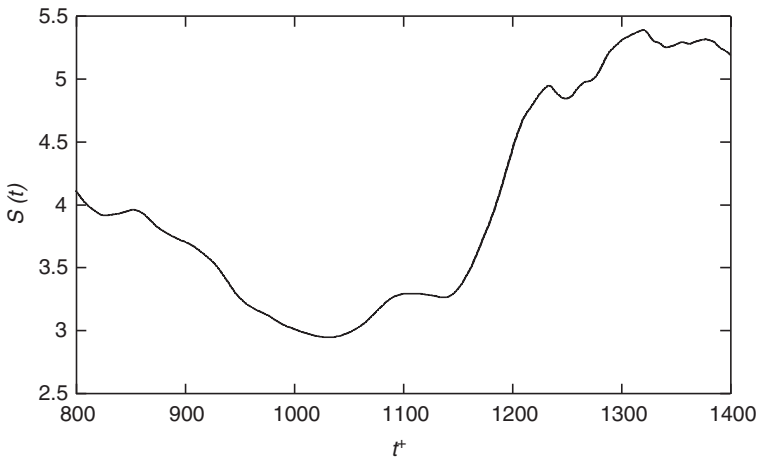

Figure 8. Representational entropy during entropy event.

may be of considerable importance in developing turbulence modification strategies and in enhancing basic understanding of the mechanism by which wall turbulence sustains itself.

5. CONCLUSIONS AND FUTURE APPLICATIONS

It has been shown that important information about the dynamics of wall bounded turbulence can be had by performing a dynamic energy balance analysis. The analysis is performed by representing the turbulent field as a sum of KL modes, each of which satisfies the boundary conditions and conserves mass. These properties simplify the resulting analysis by eliminating the pressure from the energy balance equations, along with other simplifications. The balance

equations show that all the energy in the flow must come from the applied pressure gradient acting on the net flux modes with most of the energy being transferred through the mother mode. All other modes receive energy through triad interactions which are important in understanding the dynamics. Each triad interaction determines the rate of energy transport between source and sink modes via a catalyst. Ultimately energy leaves the system through viscous dissipation.

To illustrate the effectiveness of the method, a detailed analysis of the triad interactions occurring during a turbulent burst was performed. The analysis revealed that these events are initiated by a transport of energy from the mean flow to the roll modes. As the roll modes increase in energy, they in turn transport energy to the propagating modes. The propagating modes then begin to receive energy directly from the mean flow and their energy builds as roll mode energy decreases.

The KL energy flow analysis can determine both the rate of energy transport between modes and, more importantly, the direction of energy flow. The directional information may be important in determining strategies for interfering with the turbulence, with the goal of reducing drag. For example, we have determined that during a turbulent burst, when drag increases, the energy flows first from the mean flow to the roll modes and then to the smaller scale turbulence represented by the propagating modes. This suggests the possibility that the roll modes may undergo an instability which allows the turbulence to cascade down to smaller scales. If this is the case, then stabilizing the roll modes may be one way of reducing drag. In fact, this seems to be true in the case of the phenomena associated with drag reduction by polymer addition. In this case, polymer addition reduces the bursting rate and increases roll mode energy and roll size [20–22]. Our analysis also indicates that a burst begins first with an energy exchange between the mean flow and the roll modes. This raises the question: By what physical mechanism do the roll modes extract energy from the mean? Furthermore, in a typical KL analysis, the modes are ranked according to their energy, not necessarily in order of their importance in the dynamics. The KL energy dynamics analysis developed above, however, ranks the most important non-linear interactions through the ranking of the triad transfer rates. This ranking may provide important information to those concerned with developing low-order dynamical models of such flows. For example, one may choose to include only those modes which appear in the most energetic primary and secondary triads. Pursuit of these ideas remains a goal for future work in this area.

ACKNOWLEDGEMENTS

RAH wishes to acknowledge the support of the Office of Naval Research through the Naval Research Laboratory.

APPENDIX A

A.1. Basic energy equations

The kinetic energy in the channel can be calculated by

$$E(t) = \frac{1}{2V} \int_V \mathbf{U}(\mathbf{x},t) \cdot \mathbf{U}(\mathbf{x},t)\, d\mathbf{x} \tag{A1}$$

so the rate of change of the energy in the system becomes

$$\frac{\mathrm{d}}{\mathrm{d}t}E(t)=\frac{1}{V}\int_V \mathbf{U}(\mathbf{x},t)\cdot\frac{\partial}{\partial t}\mathbf{U}(\mathbf{x},t)\,\mathrm{d}\mathbf{x} \tag{A2}$$

By using the Navier–Stokes equations, the time rate of change of the energy can be written:

$$\frac{\mathrm{d}}{\mathrm{d}t}E(t)=\frac{-1}{V}\int_V \mathbf{U}\cdot(\mathbf{U}\cdot\nabla\mathbf{U})\,\mathrm{d}\mathbf{x}-\frac{1}{V}\int_V \mathbf{U}\cdot\nabla p\,\mathrm{d}\mathbf{x} \tag{A3}$$

$$+\frac{1}{V\,Re_\tau}\int_V \mathbf{U}\cdot\nabla^2\mathbf{U}\,\mathrm{d}\mathbf{x}+\frac{1}{V}\int_V \mathbf{U}\cdot\mathbf{e}_1\,\mathrm{d}\mathbf{x} \tag{A4}$$

An examination of the fluctuating pressure term shows

$$\begin{aligned}\int_V \mathbf{U}\cdot\nabla p\,\mathrm{d}\mathbf{x}&=\int_V \nabla\cdot(p\mathbf{U})\,\mathrm{d}\mathbf{x}-\int_V p(\nabla\cdot\mathbf{U})\,\mathrm{d}\mathbf{x}\\&=\int_S \mathbf{n}\cdot(p\mathbf{U})\,\mathrm{d}S-0=0\end{aligned} \tag{A5}$$

where the surface integral is zero due to the periodic boundary conditions. A similar examination of the convection term shows

$$\begin{aligned}-\int_V \mathbf{U}\cdot(\mathbf{U}\cdot\nabla\mathbf{U})\,\mathrm{d}\mathbf{x}&=-\frac{1}{2}\int_V \nabla\cdot((\mathbf{U}\cdot\mathbf{U})\mathbf{U})\,\mathrm{d}\mathbf{x}+\frac{1}{2}\int_V(\mathbf{U}\cdot\mathbf{U})(\nabla\cdot\mathbf{U})\,\mathrm{d}\mathbf{x}\\&=-\frac{1}{2}\int_S \mathbf{n}\cdot((\mathbf{U}\cdot\mathbf{U})\mathbf{U})\,\mathrm{d}S=0\end{aligned} \tag{A6}$$

Thus the rate of change of energy is

$$\frac{\mathrm{d}}{\mathrm{d}t}E(t)=\frac{1}{V\,Re_\tau}\int_V \mathbf{U}\cdot\nabla^2\mathbf{U}\,\mathrm{d}\mathbf{x}+\frac{1}{V}\int_V \mathbf{U}\cdot\mathbf{e}_1\,\mathrm{d}\mathbf{x} \tag{A7}$$

By writing $\mathbf{U}$ in subscript notation, U_i, and using Green's first identity, the viscous term can be rewritten as

$$\int_V U_i\nabla^2 U_i\,\mathrm{d}\mathbf{x}=\int_S U_i\frac{\partial U_i}{\partial n}\,\mathrm{d}S-\int_V \nabla U_i\nabla U_i\,\mathrm{d}\mathbf{x} \tag{A8}$$

where the surface integral is zero because of the homogeneous and periodic boundary conditions and the volume integral on the right side of the equation is positive because the integrand is always greater than or equal to zero. It follows, as expected, that viscosity can only act to drain energy from the system.

A.2. Energy transfer among K-L modes

The dynamic equation for each mode is written by substituting the expansion given by Equation (12) into the Navier–Stokes equations producing

$$\sum_{\mathbf{k}'''} \frac{\mathrm{d}}{\mathrm{d}t} a^{\mathbf{k}'''}(t)\phi^{\mathbf{k}'''} = -\left(\sum_{\mathbf{k}'} a^{\mathbf{k}'}\boldsymbol{\phi}^{\mathbf{k}'}\right)\cdot\nabla\left(\sum_{\mathbf{k}''} a^{\mathbf{k}''}\boldsymbol{\phi}^{\mathbf{k}''}\right) - \nabla p + \frac{1}{R_\tau}\nabla^2\left(\sum_{\mathbf{k}'} a^{\mathbf{k}'}\boldsymbol{\phi}^{\mathbf{k}'}\right) + \mathbf{e}_1 \tag{A9}$$

A set of coupled ordinary differential equations for the coefficients $a^{\mathbf{k}}(t)$ is written by multiplying this equation by $\bar{\boldsymbol{\phi}}^{\mathbf{k}}$ and integrating over the entire domain,

$$\begin{aligned}\frac{\mathrm{d}}{\mathrm{d}t} a^{\mathbf{k}}(t) &= -\sum_{\mathbf{k}'}\sum_{\mathbf{k}''} a^{\mathbf{k}'}a^{\mathbf{k}''}\frac{1}{V}\int_V \bar{\boldsymbol{\phi}}^{\mathbf{k}}\cdot(\boldsymbol{\phi}^{\mathbf{k}'}\cdot\boldsymbol{\nabla}\boldsymbol{\phi}^{\mathbf{k}''})\,\mathrm{d}\mathbf{x} - \frac{1}{V}\int_V \bar{\boldsymbol{\phi}}^{\mathbf{k}}\cdot\nabla p\,\mathrm{d}\mathbf{x} \\ &\quad + \frac{1}{VR_\tau}\sum_{\mathbf{k}'} a^{\mathbf{k}'}\int_V \bar{\boldsymbol{\phi}}^{\mathbf{k}}\cdot\nabla^2\boldsymbol{\phi}^{\mathbf{k}'}\,\mathrm{d}\mathbf{x} + \frac{1}{V}\int_V \bar{\boldsymbol{\phi}}^{\mathbf{k}}\cdot\mathbf{e}_1\,\mathrm{d}\mathbf{x} \\ &= -\sum_{\mathbf{k}'}\sum_{\mathbf{k}''} a^{\mathbf{k}'}a^{\mathbf{k}''}\beta^{\mathbf{k}\mathbf{k}'\mathbf{k}''} + \frac{1}{R_\tau}\sum_{\mathbf{k}'} a^{\mathbf{k}'}\varepsilon^{\mathbf{k}\mathbf{k}'} + \eta^{\mathbf{k}}\end{aligned} \tag{A10}$$

As was shown previously, the integral involving the fluctuating pressure terms is zero due to the periodicity of the pressure field and the eigenfunctions, along with the fact that the eigenfunctions are incompressible and zero along the surfaces $x_2 = 1$ and -1. The time rate of change of energy for each mode can then be computed from

$$\begin{aligned}\frac{\mathrm{d}}{\mathrm{d}t} E^{\mathbf{k}}(t) &= \frac{1}{2}\left(\bar{a}^{\mathbf{k}}(t)\frac{\mathrm{d}}{\mathrm{d}t} a^{\mathbf{k}}(t)\right) \\ &= \frac{1}{2}\left(-\bar{a}^{\mathbf{k}}\sum_{\mathbf{k}'}\sum_{\mathbf{k}''} a^{\mathbf{k}'}a^{\mathbf{k}''}\beta^{\mathbf{k}\mathbf{k}'\mathbf{k}''} + \bar{a}^{\mathbf{k}}\frac{1}{R_\tau}\sum_{\mathbf{k}'} a^{\mathbf{k}'}\varepsilon^{\mathbf{k}\mathbf{k}'} + \bar{a}^{\mathbf{k}}\eta^{\mathbf{k}}\right)\end{aligned} \tag{A11}$$

Here we examine the viscous term in greater detail. The $\varepsilon^{\mathbf{k}\mathbf{k}'}$ term can be written, using the expansion given by Equation (10):

$$\begin{aligned}\varepsilon^{\mathbf{k}\mathbf{k}'} &= \frac{1}{V}\int_V \bar{\boldsymbol{\phi}}^{\mathbf{k}}\cdot\nabla^2\boldsymbol{\phi}^{\mathbf{k}'}\,\mathrm{d}\mathbf{x} \\ &= \frac{-4\pi^2}{V}\left(\frac{m'^2}{L_1^2} + \frac{n'^2}{L_3^2}\right)\left(\int_V \bar{\boldsymbol{\phi}}^{\mathbf{k}}\cdot\boldsymbol{\phi}^{\mathbf{k}'}\,\mathrm{d}\mathbf{x}\right) + \frac{1}{V}\int_V \bar{\boldsymbol{\phi}}^{\mathbf{k}}\cdot\frac{\mathrm{d}^2}{\mathrm{d}x_2^2}\boldsymbol{\phi}^{\mathbf{k}'}\,\mathrm{d}\mathbf{x}\end{aligned}$$

$$= \int_0^{L_1} \mathrm{e}^{\frac{2\pi \mathrm{i}(m'-m)x_1}{L_1}} \, \mathrm{d}x_1 \int_0^{L_3} \mathrm{e}^{\frac{2\pi \mathrm{i}(n'-n)x_3}{L_1}} \, \mathrm{d}x_3$$

$$\left(\int_{-1}^{1} \frac{-4\pi^2}{V} \left(\frac{m'^2}{L_1^2} + \frac{n'^2}{L_3^2} \right) \bar{\boldsymbol{\psi}}^q \cdot \boldsymbol{\psi}^{q'} \, \mathrm{d}x_2 + \frac{1}{V} \int_{-1}^{1} \bar{\boldsymbol{\psi}}^q \cdot \frac{\mathrm{d}^2}{\mathrm{d}x_2^2} \boldsymbol{\psi}^{q'} \, \mathrm{d}x_2 \right) \tag{A12}$$

By examining the integral in the x_1 direction and the integral in the x_3 direction, we can see that these are zero unless $m = m'$ and $n = n'$, i.e. a mode only has viscous interaction with another mode with the same wave number. The last line of the equations shows two integrals in the x_2 direction. In the case $\mathbf{k} = \mathbf{k}'$, the first of these integrals will be real and non-positive since the eigenfunctions are orthogonal. In this case, the second integral can be rewritten as

$$\int_{-1}^{1} \bar{\boldsymbol{\psi}}^q \cdot \frac{\mathrm{d}^2}{\mathrm{d}x_2^2} \boldsymbol{\psi}^q \, \mathrm{d}x_2 = \bar{\boldsymbol{\psi}}^q \cdot \frac{\mathrm{d}}{\mathrm{d}x_2} \boldsymbol{\psi}^q \Big|_{-1}^{1} - \int_{-1}^{1} \overline{\frac{\mathrm{d}}{\mathrm{d}x_2} \boldsymbol{\psi}^q} \cdot \frac{\mathrm{d}}{\mathrm{d}x_2} \boldsymbol{\psi}^q \, \mathrm{d}x_2 \tag{A13}$$

Because the first term in (A13) is zero due to the boundary conditions, and the integrand of the second term is real and negative, the integral on the left is real and negative, so the value of $\varepsilon^{\mathbf{kk}}$ must also be real and negative. It therefore follows, as expected, that viscosity can only act to drain energy from a given mode.

Energy moves from the net flux modes to the higher order modes through the convection terms which we represent through the terms $\beta^{\mathbf{kk'k''}}$. While the $\varepsilon^{\mathbf{kk'}}$ terms produced a complex exponential with $m' - m$ and $n' - n$ in the numerator, the integral for the $\beta^{\mathbf{kk'k''}}$ terms will produce a complex exponential with $m' + m'' - m$ and $n' + n'' - n$ in the numerator. Just as in the $\varepsilon^{\mathbf{kk'}}$ terms, the $\beta^{\mathbf{kk'k''}}$ terms will be zero unless m', m'' and $-m$ add to zero as well as n', n'' and $-n$. When these two conditions are met, the modes are said to form a *triad*. While convection can have no effect on the net energy change of the system, it can have an effect on the energy distribution among modes—that is, it can move energy among the K-L modes.

The rate of energy transport due to a triad interaction can be written:

$$\left(\frac{\mathrm{d}}{\mathrm{d}t} E^{\mathbf{k}}(t) \right)_{\beta^{\mathbf{kk'k''}}} = \frac{1}{2} (-\bar{a}^{\mathbf{k}} a^{\mathbf{k'}} a^{\mathbf{k''}} \beta^{\mathbf{kk'k''}}) \tag{A14}$$

In taking a closer look at the triads, we note that if $\mathbf{kk'k''}$ forms a triad in the energy equation for the $\mathbf{k}$ mode, then $\mathbf{k''\bar{k}'k}$ forms a triad in the energy equation for the $\mathbf{k''}$ mode ($\bar{\mathbf{k}}'$ refers to the triplet $(-m', -n', q)$). This rate of energy change can be written as

$$\left(\frac{\mathrm{d}}{\mathrm{d}t} E^{\mathbf{k''}}(t) \right)_{\beta^{\mathbf{k''\bar{k}'k}}} = \frac{1}{2} (-\bar{a}^{\mathbf{k''}} a^{\bar{\mathbf{k}}'} a^{\mathbf{k}} \beta^{\mathbf{k''\bar{k}'k}}) \tag{A15}$$

Because this derivative is real, it is equal to its own complex conjugate. In addition, because the flow is real, the coefficients have the property $a^k = \bar{a}^{\bar{k}}$, so the time derivative can be rewritten as

$$\left(\frac{\mathrm{d}}{\mathrm{d}t} E^{\mathbf{k''}}(t) \right)_{\beta^{\mathbf{k''\bar{k}'k}}} = \frac{1}{2} (\overline{-\bar{a}^{\mathbf{k''}} a^{\bar{\mathbf{k}}'} a^{\mathbf{k}} \beta^{\mathbf{k''\bar{k}'k}}}) = \frac{1}{2} (-\bar{a}^{\mathbf{k}} a^{\mathbf{k'}} a^{\mathbf{k''}} \bar{\beta}^{\mathbf{k''\bar{k}'k}}) \tag{A16}$$

We compare the terms $\beta^{\mathbf{k}\mathbf{k}'\mathbf{k}''}$ and $\bar{\beta}^{\mathbf{k}''\bar{\mathbf{k}}'\mathbf{k}}$ by examining the equation

$$\int_V \nabla\cdot((\bar{\boldsymbol{\phi}}^{\mathbf{k}}\cdot\boldsymbol{\phi}^{\mathbf{k}''})\boldsymbol{\phi}^{\mathbf{k}'})\,\mathrm{d}\mathbf{x} = \int_V (\nabla\cdot\boldsymbol{\phi}^{\mathbf{k}'})(\bar{\boldsymbol{\phi}}^{\mathbf{k}}\cdot\boldsymbol{\phi}^{\mathbf{k}''})\,\mathrm{d}\mathbf{x} + \int_V \bar{\boldsymbol{\phi}}^{\mathbf{k}}\cdot(\boldsymbol{\phi}^{\mathbf{k}'}\cdot\nabla\boldsymbol{\phi}^{\mathbf{k}''})\,\mathrm{d}\mathbf{x} + \int_V \boldsymbol{\phi}^{\mathbf{k}''}\cdot(\boldsymbol{\phi}^{\mathbf{k}'}\cdot\nabla\bar{\boldsymbol{\phi}}^{\mathbf{k}})\,\mathrm{d}\mathbf{x}$$

The integral on the left can be converted to a surface integral which is zero due to the periodic and no slip boundary conditions. The first integral on the right is zero due to the incompressibility of the eigenfunctions. This leaves the result

$$\int_D \bar{\boldsymbol{\phi}}^{\mathbf{k}}\cdot(\boldsymbol{\phi}^{\mathbf{k}'}\cdot\nabla\boldsymbol{\phi}^{\mathbf{k}''})\,\mathrm{d}\mathbf{x} = -\int_D \boldsymbol{\phi}^{\mathbf{k}''}\cdot(\boldsymbol{\phi}^{\mathbf{k}'}\cdot\nabla\bar{\boldsymbol{\phi}}^{\mathbf{k}})\,\mathrm{d}\mathbf{x} \text{ or } \beta^{\mathbf{k}\mathbf{k}'\mathbf{k}''} = -\bar{\beta}^{\mathbf{k}''\bar{\mathbf{k}}'\mathbf{k}}$$

which shows that the energy change in the modes $\mathbf{k}$ and $\mathbf{k}'$ due to these triads can be written as

$$\left(\frac{\mathrm{d}}{\mathrm{d}t}E^{\mathbf{k}}(t)\right)_{\beta^{\mathbf{k}\mathbf{k}'\mathbf{k}''}} = -\left(\frac{\mathrm{d}}{\mathrm{d}t}E^{\mathbf{k}''}(t)\right)_{\beta^{\mathbf{k}''\bar{\mathbf{k}}'\mathbf{k}}} \tag{A17}$$

Thus the energy which flows out of the mode $\mathbf{k}$ through this triad flows into the $\mathbf{k}''$ term and vice versa. We conclude from this analysis that we can determine the rate of energy change for each mode, and we can determine where the energy is coming from and going to.

The magnitude of the triad is measured by the time average of the energy flow,

$$T^{\mathbf{k}\mathbf{k}'\mathbf{k}''} = \frac{1}{2T}\left(\int_0^T -\bar{a}^{\mathbf{k}}a^{\mathbf{k}'}a^{\mathbf{k}''}\beta^{\mathbf{k}\mathbf{k}'\mathbf{k}''}\,\mathrm{d}t\right) = \frac{1}{2}(\langle -\bar{a}^{\mathbf{k}}a^{\mathbf{k}'}a^{\mathbf{k}''}\rangle\beta^{\mathbf{k}\mathbf{k}'\mathbf{k}''}) \tag{A18}$$

If $T^{\mathbf{k}\mathbf{k}'\mathbf{k}''}$ is greater than zero, then the mean effect of this triad is to move energy from the $\mathbf{k}''$ mode to the $\mathbf{k}$ mode. In this case we report the $\mathbf{k}''$ mode to be the *source* mode and the $\mathbf{k}$ mode to be the *sink* mode. If $T^{\mathbf{k}\mathbf{k}'\mathbf{k}''}$ is negative, $\mathbf{k}$ is the source mode and $\mathbf{k}''$ is the sink mode. No energy comes from or goes to the $\mathbf{k}'$ term through this triad meaning that it acts as a *catalyst*. The total change of energy from the triads can be calculated by a sum over the terms given by $T^{\mathbf{k}\mathbf{k}'\mathbf{k}''}$. Because we have shown that for each triad, there is exactly one triad of equal magnitude and opposite sign, the sum over these triads is zero. This finding is in line with the fact that convection does not produce or consume energy.

REFERENCES

1. Kline SJ, Reynolds WC, Shraub FA, Runstadler PW. The structure of turbulent boundary layers. *Journal of Fluid Mechanics* 1967; **30**:741–773.
2. Robinson SK. Coherent motions in the turbulent boundary layer. *Annual Review of Fluid Mechanics* 1991; **23**:601–639.
3. Moin P, Moser RD. Characteristic eddy decomposition of turbulence in a channel. *Journal of Fluid Mechanics* 1989; **200**:471–509.
4. Sirovich L, Ball KS, Keefe LR. Plane waves and structures in turbulent channel flow. *Physics of Fluids A* 1990; **2**:2217–2226.
5. Sirovich L, Ball KS, Handler RA. Propagating structures in wall bounded turbulent flow. *Theoretical Computations in Fluid Dynamics* 1991; **2**:307–317.

6. Aubry N, Holmes P, Lumley JL, Stone E. The dynamics of coherent structures in the wall region of a turbulent boundary layer. *Journal of Fluid Mechanics* 1988; **192**:115–173.
7. Zhou X, Sirovich L. Coherence and chaos in a model of the turbulent boundary layer. *Physics of Fluids A* 1992; **4**:2855–2874.
8. Sirovich L, Xhou X. Dynamical model of wall bounded turbulence. *Physical Review Letters* 1994; **72**:340–343.
9. Webber GA, Handler RA, Sirovich L. The Karhunen Loeve decomposition of minimal channel flow. *Physics of Fluids* 1997; **9**:1054–1066.
10. Jimenez J, Moin P. The minimal flow unit in near-wall turbulence. *Journal of Fluid Mechanics* 1991; **225**: 213–240.
11. Dean RB. Reynolds number dependence of skin friction and other bulk flow variables in two dimensional rectangular duct flow. *Journal of Fluids Engineering Transactions of ASME* 1978; **100**:215–223.
12. Kim J, Moin P, Moser R. Turbulence statistics of turbulent channel flow at low Reynolds number. *Journal of Fluid Mechanics* 1987; **177**:133–166.
13. Handler RA, Hendricks EW, Leighton RI. Low Reynolds number calculation of turbulent channel flow: a general discussion. Naval Research Laboratory Memorandum Report 6410, 1989.
14. Lumley JL. *Stochastic Tools in Turbulence*. Academic: New York, 1970.
15. Preisendorfer RW. *Principal Component Analysis in Meteorology and Oceanography*. Elsevier: New York, 1988.
16. Sirovich L. Turbulence and the dynamics of coherent structures. *Quarterly of Applied Mathematics* 1987; **45**:561–590.
17. Smith CR, Metzler SP. The characteristics of low speed streaks in the near wall region of a turbulent boundary layer. *Journal of Fluid Mechanics* 1983; **129**:27–54.
18. Brooke JW, Hanratty TJ. Origin of turbulence producing eddies in a channel flow. *Physics of Fluids A* 1993; **5**:1011–1022.
19. Bernard PS, Thomas JT, Handler RA. Vortex dynamics and the production of Reynolds stress. *Journal of Fluid Mechanics* 1993; **253**:385–419.
20. Bogard DG, Tiederman WG. Burst detection with single point velocity measurements. *Journal of Fluid Mechanics* 1986; **162**:389–413.
21. Sureshkummar R, Beris AN, Handler RA. Direct numerical simulation of the turbulent channel flow of a polymer solution. *Physics of Fluids* 1997; **9**:743–755.
22. Handler RA, Levich E, Sirovich L. Drag reduction in turbulent channel flow by phase randomization. *Physics of Fluids A* 1993; **5**:686–694.

